Comparison of refraction information extraction methods in diffraction enhanced imaging

Chunhong Hu,[1,2] Lu Zhang,[1] Hui Li,[1] and Shuqian Luo[1,*]

[1]*College of Biomedical Engineering, Capital Medical University, Beijing 100069, China*
[2]*National Laboratory of Pattern Recognition, Institute of Automation, Chinese Academy of Sciences, Beijing 100080, China*
[*]*Corresponding author: sqluo@ieee.org*

Abstract: Diffraction enhanced imaging (DEI) is a powerful phase-sensitive technique that generates the improved contrast of weakly absorbing samples compared to conventional radiography. The x-ray refraction contrast of the sample is an important contrast in DEI, and it vastly exceeds the absorption contrast for weakly absorbing samples imaging, which makes it hold great promise for medical, biological and material applications. In order to effectively utilize the refraction contrast, the key procedure is first to obtain the refraction information expressed as the refraction image. By comparing the signal-to-noise ratio (SNR) of the refraction image, x-ray radiation dose of the sample and the range of obtained refraction angles, the different refraction information extraction methods are investigated in this paper, and the experimental results confirm the conclusion.

OCIS codes: (340.7440) X-ray imaging; (340.6720) Synchrotron radiation; (120.5710) Refraction; (100.5070) Phase retrieval; (170.3880) Medical and biological imaging.

References and links

1. T. J. Davis, D. Gao, T. E. Gureyev, A. W. Stenvenson and S. W. Wilkins, "Phase-contrast imaging of weakly absorbing materials using hard x-rays," Nature **373**, 595-598 (1995).
2. A. Momose, T. Takeda, Y. Itai, and K. Hirano, "Phase-contrast x-ray computed tomography for observing biological soft tissues," Nat. Med. **2**, 473-475 (1996).
3. D. Chapman, W. Thomlinson, R. E. Johnston, D. Washburn, E. Pisano, N. Gmur, Z. Zhong, F. Arfelli, and D. Sayers, "Diffraction enhanced x-ray imaging," Phys. Med. Biol. **42**, 2015-2025 (1997).
4. M. N. Wernick, O. Wirjadi, D. Chapman, Z. Zhong, N. P. Galatsanos, Y. Y. Yang, J. G. Brankov, O. Oltulu, M. A. Anastasion, and C. Muehleman, "Multiple-image radiography," Phys. Med. Biol. **48**, 3875-3895 (2003).
5. E. Pagot, P. Cloetens, S. Fiedler, A. Bravin, P. Coan P, J. Baruchel, J. Hartwig, and W. Thomlinson W, "A method to extract quantitative information in analyzer-based x-ray phase contrast imaging," Appl. Phys. Lett. **82**, 3421-3423 (2003).
6. O. Oltulu, Z. Zhong, M. Hasnah, and D. Chapman, "Extraction of extinction, refraction and absorption properties in diffraction enhanced imaging," J. Phys. D: Appl. Phys. **36**, 2152-2156 (2003).
7. J. G. Brankov, M. N. Wernick, Y. Y. Yang, J. Li, C. Muehleman, Z. Zhong, and M. A. Anastasion, "Computed tomography implementation of multiple-image radiography," Med. Phys. **33**, 278-289 (2006).
8. C. Muehleman, J. Li, Z. Zhong, J. G. Brankov, and M. N. Wernick, "Multiple-image radiography for human soft tissue," J. Anat. **208**, 115-124 (2006).
9. C. L. Liu, X. H. Yan, X. Y. Zhang, W. T. Yang, W. J. Peng, D. R. Shi, P. P. Zhu, W. X. Huang, and Q. X. Yuan, "Evaluation of x-ray diffraction enhanced imaging in the diagnosis of breast cancer," Phys. Med. Biol. **52**, 419-427 (2007).
10. G. Li, N. Wang, and Z. Y. Wu, "Hard x-ray diffraction enhanced imaging only using two crystals," Chin. Sci. Bull. **49**, 2120-2125 (2004).
11. Z. F. Huang, K. J. Kang, and Z. Li, "Refraction-angle resolution of diffraction enhanced imaging," Phys. Med. Biol. **51**, 3031-3039 (2006).
12. M. Z. Kiss, D. E. Sayers, and Z. Zhong, "Measurement of image contrast using diffraction enhanced imaging," Phys. Med. Biol. **48**, 325-340 (2003).

#99011 - $15.00 USD Received 24 Jul 2008; revised 18 Sep 2008; accepted 29 Sep 2008; published 6 Oct 2008

1. Introduction

The conventional radiography derives contrast from differences in x-ray absorption. For weakly absorbing samples such as biological soft tissues, polymers and so on, however, conventional radiography may achieve low contrast and spatial resolution. X-ray phase-contrast imaging (PCI) is a new emerging imaging technique that exploits a contrast mechanism based on differences in the x-ray refractive index distribution of a sample [1, 2]. Compared with the conventional radiography, PCI can offer higher contrast and spatial resolution for weakly absorbing samples, and can clearly display their inner structures [2].

Diffraction enhanced imaging (DEI) is one of the different PCI techniques, and it has been widely studied and applied by scientists in many fields. DEI can generate contrast from a sample's x-ray absorption, refraction and ultra-small angle x-ray scattering (USAXS) properties, and it utilizes an analyzer crystal with high angular sensitivity to measure the three contrasts, which dramatically improves the contrast and spatial resolution of the images [3]. Among these contrasts, the refraction contrast is very important, and it is more sensitive to density variations of the weakly absorbing samples than the absorption contrast. In order to effectively utilize the x-ray refraction contrast of the sample, it need first obtain the refraction information expressed as the refraction image. Recently, the refraction information extraction becomes a hot issue in DEI [3-7], and attains widespread studies and applications in biological and medical fields, such as breast cancer diagnosis, cartilage imaging, and so on [4, 7-9]. In this paper, different refraction information extraction methods are investigated and compared, and the experiments are utilized to validate the conclusion.

2. Principle of DEI

The DEI setup is sketched in Fig. 1, and it is composed of two perfect crystals' monochromator-analyzer system with a sample placed between them [10]. The monochromator crystal is used to generate a nearly monochromatic x-ray beam. Then the monochromatic beam transmitted through the sample is incident upon the analyzer crystal, and the intensity of the x-ray beam reflected by the analyzer crystal is measured by a detector [3]. The rocking curve (RC) of DEI system describes the reflectivity of the analyzer crystal as a function of the incident angle, as shown in Fig. 2, and the triangle labels indicate the selected points on the RC in DEI imaging. The full width half maximum (FWHM) of the RC is about a few micro-radians, which is approximately equal to Darwin width (w_D) of the crystal, so the analyzer crystal has a high angular sensitivity. The diffracted intensity is picked up by setting the angle of analyzer crystal, and the observed DEI intensity can be given by

$$I = I_R R(\theta + \Delta\theta), \tag{1}$$

where $R(\theta)$ is the analyzer reflectivity, namely the RC, θ is the setting angle of analyzer crystal, I_R is the apparent absorption intensity, and $\Delta\theta$ is the refraction angle of the x-ray passed through the sample.

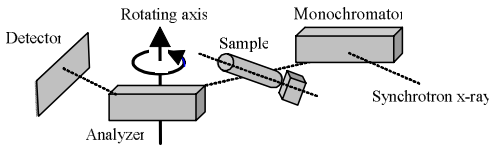

Fig. 1. The DEI setup

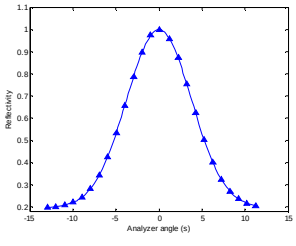

Fig. 2. The RC of DEI system in the experiment

#99011 - $15.00 USD Received 24 Jul 2008; revised 18 Sep 2008; accepted 29 Sep 2008; published 6 Oct 2008

3. Refraction information extraction methods

When the x-ray penetrates through a sample, the interaction of x-ray with the sample can be expressed by the complex refractive index, $n = 1 - \delta + i\beta$. The real part δ denotes the phase change of the x-ray due to the refraction, and the imaginary part β corresponds to the absorption. For the weakly absorbing samples, the values of δ can be several orders of magnitude larger than β terms, which makes the refraction contrast greatly exceed the absorption contrast.

In Eq. (1), $R(\theta + \Delta\theta)$ can be expressed by the Taylor expansion

$$R(\theta + \Delta\theta) = R(\theta) + \frac{dR}{d\theta}(\theta)\Delta\theta + \varphi(\theta, \Delta\theta), \tag{2}$$

where

$$\varphi(\theta, \Delta\theta) = \sum_{n=2}^{\infty} \frac{1}{n!} R^{(n)}(\theta)(\Delta\theta)^n . \tag{3}$$

The $R^{(n)}(\theta)$ in Eq. (3) denotes n-th derivative of $R(\theta)$. Because the slope of the rocking curve is fairly constant at $\theta = \pm w_D/2$, Eq. (2) can be approximated by a first-order Taylor expansion for small values of $\Delta\theta$. That is

$$R(\theta + \Delta\theta) = R(\theta) + \frac{dR}{d\theta}(\theta)\Delta\theta . \tag{4}$$

According to Eqs. (3) and (4), the accuracy of approximation is well enough for smaller refractions in the sample, but it can lead to sizeable errors with the increase of the refractions. Combining Eqs. (1) and (4), the refraction image, namely the refraction angle image ($\Delta\theta$) can be calculated using two DEI images (I_L, I_H) at $\theta_L = -w_D/2$ and $\theta_H = w_D/2$ with respect to the center of the RC [3]. That is,

$$\Delta\theta = \frac{I_H R(\theta_L) - I_L R(\theta_H)}{I_L \left(\frac{dR}{d\theta}\right)(\theta_H) - I_H \left(\frac{dR}{d\theta}\right)(\theta_L)} . \tag{5}$$

Actually, the RC of DEI system can be well fitted by a Gaussian function, so $R(\theta)$ can be expressed as

$$R(\theta) = A\exp\left(\frac{-\theta^2}{2\sigma^2}\right), \tag{6}$$

where $w_D = 2\sigma(2\ln 2)^{1/2}$ and A is the area of the RC. By use of the characteristics of the Gaussian function, we can obtain

$$R(\theta_L) = R(\theta_H) \ , \ (dR/d\theta)(\theta_L) = -(dR/d\theta)(\theta_H) . \tag{7}$$

Thus, Eq. (5) can be expressed as

$$\Delta\theta = \frac{w_D}{4\ln 2}\frac{I_L - I_H}{I_L + I_H} . \tag{8}$$

#99011 - $15.00 USD Received 24 Jul 2008; revised 18 Sep 2008; accepted 29 Sep 2008; published 6 Oct 2008

From Eq. (8), we can see that the maximum value of $|\Delta\theta|$ is $w_D/(4\ln 2)$, and any refraction angle of more than the maximum value can not be calculated [11]. Actually, the first-order Taylor approximation of the RC in essence limits the range of obtained refraction angles in this method.

Based on Eq. (6), $R(\theta+\Delta\theta)$ in Eq. (1) can be expressed as

$$R(\theta+\Delta\theta)=A\exp\left(\frac{-(\theta+\Delta\theta)^2}{2\sigma^2}\right). \tag{9}$$

Compared with Eq. (4), Eq. (9) can overcome the first-order Taylor approximation of the RC. In addition, Eq. (4) generally requires the angle θ to be set at $-w_D/2$ or $w_D/2$. However, Eq. (9) does not impose so strong a requirement, and thus it provides more flexibility in the choice of the angle θ. Using Eqs. (1) and (9), the intensities of the images taken at θ_L and θ_H can be expressed as follows

$$I_{L,H}=I_R A\exp\left(\frac{-(\theta_{L,H}+\Delta\theta)^2}{2\sigma^2}\right). \tag{10}$$

Based on Eq. (10), a new method is presented to obtain the refraction image. That is

$$\Delta\theta=\frac{w_D}{8\ln 2}\ln\left(\frac{I_L}{I_H}\right). \tag{11}$$

Obviously, the values of I_H in Eq. (11) can not be equal to zero, so it need preprocess prior to calculation when gray values of the pixels are equal to zero. Among numerous preprocessing methods, the simplest can be performed by setting gray values of these pixels one. For the DEI image with 0-255 grayscale range, the grayscale range of I_H can be expressed as 1-255 after the above preprocessing. Thus, from Eq. (11), we can obtain that the maximum value of $|\Delta\theta|$ is approximately w_D. Comparison between Eqs. (8) and (11) shows that Eq. (11) can effectively extend the range of calculated refraction angles. Moreover, the range will also increase with the increase of the grayscale range of DEI image.

The refraction image can be calculated by use of either of Eqs. (8) and (11), and furthermore, both the calculation methods need just two DEI images, which decreases the imaging time and x-ray radiation dose of the sample. Multiple image radiography (MIR) is a significant development over DEI based on a statistical analysis, and it can produce true absorption, refraction and USAXS images, respectively [4-7]. Compared with the above two methods, MIR method is more robust to noise and produces more accurate refraction image, but it simultaneously increases x-ray radiation dose of the sample. In MIR, two series of images are acquired in N ($N \geq 3$) positions of the RC, one with sample and one without sample, and they give respectively, for each individual pixel, a sample RC and a background RC. $I_s(\theta_n)(n=1,2,...,N)$ denotes the intensity of the image in the position θ_n of the RC with the sample. $I_b(\theta_n)$ denotes the intensity of the image in the position θ_n of the RC without the sample. Then the refraction image can be expressed as follows

#99011 - $15.00 USD Received 24 Jul 2008; revised 18 Sep 2008; accepted 29 Sep 2008; published 6 Oct 2008

$$\Delta\theta = \frac{\sum_{n=1}^{N} I_{\mathrm{s}}(\theta_n)\theta_n}{\sum_{n=1}^{N} I_{\mathrm{s}}(\theta_n)} - \frac{\sum_{n=1}^{N} I_{\mathrm{b}}(\theta_n)\theta_n}{\sum_{n=1}^{N} I_{\mathrm{b}}(\theta_n)}. \tag{12}$$

For the refraction images described by Eqs. (8), (11) and (12), the signal-to-noise ratio (SNR) can be defined based on the noise level in the background. That is

$$\mathrm{SNR} = \left(\theta_{\mathrm{R,max}} - \theta_{\mathrm{R,min}}\right) \Big/ \sigma_{\mathrm{ref}} , \tag{13}$$

where $\theta_{\mathrm{R,max}}$ and $\theta_{\mathrm{R,min}}$ are the maximum and minimum values in the refraction image respectively, and σ_{ref} is a standard deviation of the refraction signal from the average background [12].

4. Experimental results

The experiments were performed at the 4W1A beamline of Beijing Synchrotron Radiation Facilities (BSRF). As shown in Fig. 1, The double-crystal DEI setup was used in the experiments. Two perfect Si(111) crystals were used as monochromator and analyzer. The x-ray beam energy was set at 9.4 keV. The detector employed an x-ray FDI-18mm camera system (Photonic Science Ltd.) with 1300×1030 pixels, and 10.9×10.9 μm^2 per pixel. The guinea pig cochlea was selected as the sample.

The cochlea is a very complex micro-organ with unique function of generating hearing, which is attributed to its peculiar structural arrangement. The cochlear morphologic research is always the basis of hearing research. In this paper, the DEI technique was applied to the guinea pig cochlea imaging, and the acquired images were used to calculate the refraction image. Table 1 shows the ranges of refraction angles in the refraction images of the guinea pig cochlea, and the refraction images are calculated by Eqs. (8), (11) and (12), respectively. Note that the refraction image calculated by Eq. (12) was based on a 25-image series. For simplicity, DEI, EDEI and MIR in Table 1 denote the refraction information extraction methods that are based on Eqs. (8), (11) and (12) respectively. Obviously, a greater range of the refraction angles using the EDEI method can be obtained compared with the DEI method, and the MIR method vastly improves the range of the refraction angles.

Table 1.The range of refraction angles in the refraction images of the guinea pig cochlea obtained using different refraction information extraction methods

Refraction angle	DEI	EDEI	MIR
maximum	2.4089s	3.1286s	6.4417s
minimum	-2.2639s	-2.8191s	-4.6897s

As an improvement on DEI method, EDEI method is used to further compare with MIR method using SNR of the refraction image and x-ray radiation dose of the sample. Figs. 3(a) and (b) respectively show SNR and exposure time of the refraction image of the guinea pig cochlea as a function of the image number. Note that the exposure time of the refraction image is the cumulative sum of the exposure time of images that are used to calculate the refraction image. As we all know, when the energy of the x-ray beam remains constant, x-ray radiation dose of the sample is in the direct ratio to exposure time. Because all images were acquired in the same energy, the exposure time can be used to indicate relative x-ray radiation dose of the sample. In Figs. 3(a) and 3(b), the solid triangle label indicates SNR and exposure time of the refraction image in MIR method for the different image number series respectively, and the solid square label indicates SNR and exposure time of the refraction image obtained using EDEI method respectively. From Figs. 3(a) and 3(b), we can see that

#99011 - $15.00 USD Received 24 Jul 2008; revised 18 Sep 2008; accepted 29 Sep 2008; published 6 Oct 2008

SNR and exposure time of the refraction image in MIR method increase with the increase of image number, and a better SNR with less exposure time is found in the refraction image calculated using EDEI method, which is very important in biomedical imaging applications. Figs. 4(a) and (b) show the refraction images of the guinea pig cochlea, and they are obtained by use of EDEI and MIR methods respectively. The refraction image in Fig. 4(b) was calculated by MIR method based on a 25-image series. Although Fig. 4(b) has higher SNR than Fig. 4(a), they can both clearly display the holistic spiral structures and inner details of the guinea pig cochlea. According to anatomy knowledge of the inner ear and the atlas of inner ear, we can discern more micro-structures of the guinea pig cochlea such as modiolus, spiral lamina and so on. As expected, the refraction image shows a marked edge enhancement effect and results in a three-dimensional appearance, as shown in Figs. 4(a) and 4(b).

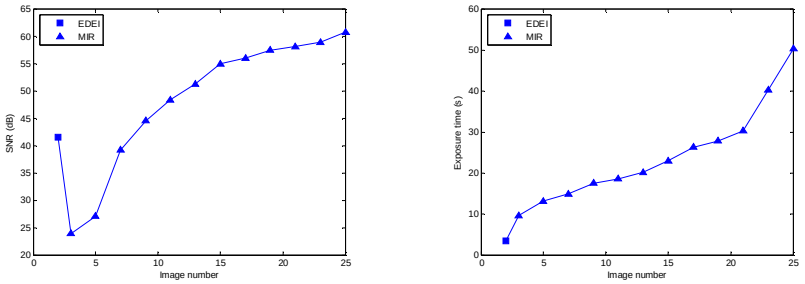

(a) (b)

Fig. 3. SNR (a) and exposure time (b) in the refraction image as a function of the image number. In (a) and (b), the solid triangle label indicates SNR and exposure time of the refraction image in MIR method for the different image number series respectively, and the solid square label indicates SNR and exposure time of the refraction image obtained using EDEI method respectively.

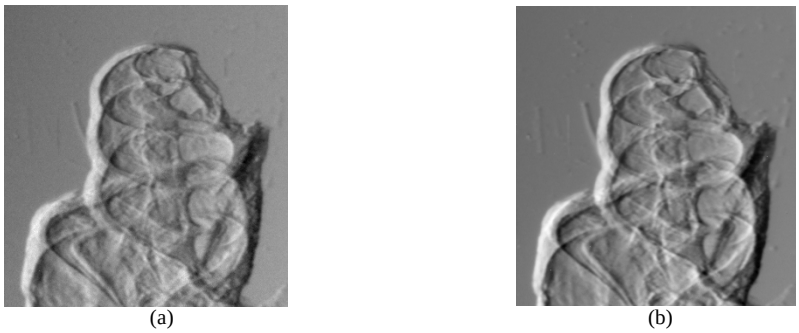

(a) (b)

Fig. 4. The refraction images of the guinea pig cochlea obtained by use of different methods: (a) EDEI and (b) MIR.

As shown above, EDEI method is a good choice in biomedical imaging applications when fully considering x-ray radiation dose of the sample, SNR of the refraction image and the obtained range of refraction angles. Of course, for the samples, such as polymers or fiber composites, their x-ray radiation doses do not have to be taken into too much consideration, and thus the long image series can be utilized to obtain the refraction image with a high SNR based on the MIR method.

5. Conclusion

The refraction image has higher contrast and spatial resolution than conventional radiograph for the weakly absorbing samples and thus it attains widespread applications in biological and medical fields. The refraction information extraction methods were compared and investigated in this paper. A method is presented to improve the original information extraction method that is based on a first-order Taylor approximation of the RC, and it can effectively extend the

#99011 - $15.00 USD Received 24 Jul 2008; revised 18 Sep 2008; accepted 29 Sep 2008; published 6 Oct 2008

range of calculated refraction angles. Moreover, the proposed method can obtain a better refraction image and can decrease the exposure time of the sample due to the need of just two DEI images. Thus, it is a good choice in biomedical imaging applications compared with MIR method. MIR method vastly improves the range of the calculated refraction angles. The SNR of the refraction image in MIR method increases with the increase of the image number per series, but this simultaneously increases the imaging time and x-ray radiation dose of the sample.

Acknowledgments

The research was supported by the National Natural Science Foundation of China (60532090 and 30770593) and the National Laboratory of Pattern Recognition, Institute of Automation, Chinese Academy of Sciences, China (07-21-9). The authors thank Prof. Zhu Peiping, Dr. Yuan Qingxi, Dr. Huang Wanxia from BSRF for assistance in our experiments.

#99011 - $15.00 USD Received 24 Jul 2008; revised 18 Sep 2008; accepted 29 Sep 2008; published 6 Oct 2008